MOTION CLOSE TO THE HOPF BIFURCATION OF THE VERTICAL FAMILY OF PERIODIC ORBITS OF L_4

MERCÈ OLLÉ, JOAN R. PACHA and JORDI VILLANUEVA
Departament de Matemàtica Aplicada I, Universitat Politècnica de Catalunya Diagonal 647, 08028 Barcelona, Spain, e-mail: merce.olle@upc.es; {joanr; jordi}@vilma.upc.es

(Received: 31 October 2003; revised: 26 March 2004 accepted: 26 February 2004)

Abstract. The paper deals with different kinds of invariant motions (periodic orbits, $2D$ and $3D$ invariant tori and invariant manifolds of periodic orbits) in order to analyze the Hamiltonian direct Hopf bifurcation that takes place close to the Lyapunov vertical family of periodic orbits of the triangular equilibrium point L_4 in the $3D$ restricted three-body problem (RTBP) for the mass parameter, μ, greater than (and close to) μ_R (Routh's mass parameter). Consequences of such bifurcation, concerning the confinement of the motion close to the hyperbolic orbits and the $3D$ nearby tori are also described.

Key words: Hopf bifurcation, invariant manifolds, invariant tori, periodic orbits, restricted problem

1. Introduction

Our framework is the spatial circular restricted three-body problem (RTBP from now on) as a Hamiltonian system of three degrees of freedom. This paper deals with the motion close to the so called vertical family of periodic orbits of the triangular points L_4 and L_5 of the RTBP.

Actually, there are several works devoted to the vertical family for values of the mass parameter μ with $\mu < \mu_R$ (the Routh critical value) – we mention (Zagouras, 1985; Castella and Jorba, 2000; Gómez et al., 2001; Jorba, 2001) and references therein – but not as many for $\mu > \mu_R$ (see for instance Jorba and Villanueva, 1997). Thus, in this work, we will concentrate on the case $\mu > \mu_R$ (but close to μ_R), and we will study the motion related to the Hopf bifurcation of the vertical family which appears if we consider a mass parameter $\mu > \mu_R$ and we follow the family for big enough amplitudes.

This bifurcation takes place when a one parameter family of periodic orbits, of a Hamiltonian system with three degrees of freedom, undergoes a transition from stability to complex instability by means of a collision of characteristic multipliers in the unit circle. According to the value of the characteristic multipliers at the collision, we will distinguish between rational and irrational collision, and according to the effect of the nonlinear terms of the Hamiltonian, the bifurcation can be direct or inverse. In the case of the

Celestial Mechanics and Dynamical Astronomy **90:** 89–109, 2004.

vertical family the bifurcation has always direct character, which means that stable objects (periodic orbits in the rational case and $2D$ tori in the irrational one) bifurcate on the unstable side (around complex unstable periodic orbits).

In this paper, we will consider different kinds of 'invariant motions' close to the critical periodic orbit in order to analyze the Hopf bifurcation (both rational and irrational cases). More precisely, we will consider periodic orbits, $2D$ and $3D$ invariant tori and the unstable and stable invariant manifolds of the hyperbolic periodic orbits. These objects will be used to show, near the bifurcation, the strong confinement of the solutions close to the invariant manifolds of the hyperbolic periodic orbits, due to the approximate coincident character of the stable and unstable manifolds.

Actually the Hopf bifurcation for a Hamiltonian system of three degrees of freedom has been analyzed (both numerically and analytically) by several authors, either considering the Hamiltonian itself or a one parameter family of $4D$ symplectic mappings having a fixed point undergoing a Hopf bifurcation for a critical value of the parameter (for example, a suitable Poincaré map of the Hamiltonian using the energy as a parameter). More precisely, their analytical approach consists in considering the Hamiltonian (the mapping) around the transition periodic orbit (fixed point for the critical value) and reduce it to a normal form up to a finite order plus a remainder; afterwards, they analyze the dynamics from the truncated normal form (which turns out to be integrable).

In the context of symplectic mappings, we mention Bridges and Furter, (1993) for an analysis of the rational collision and Bridges et al. (1994) for the irrational one – from an analytical point of view – and Pfenniger (1985), Ollé (2000), Jorba and Ollé (2004) and – from a numerical one. Concerning the Hamiltonian itself and the irrational collision situation, we refer first to (Heggie, 1985), where the normal form of the Hamiltonian, around the critical orbit, is obtained up to degree four. An analytical and complete treatment of this case has been recently carried out in (Pacha, 2002) (see also Ollé et al., 2001, 2003). In (Pacha, 2002) a tricky algorithm to transform the Hamiltonian to normal form up to an arbitrary (finite) order is described, giving also quantitative estimates of the remainder (not in normal form) as function of the normalizing order and the distance to the critical orbit. The normal form is used to give an approximate description of the dynamics, and the bounds for the remainder are used to prove the existence of a Cantor family of bifurcating $2D$ tori (with big relative measure) when the whole (non integrable) Hamiltonian is considered. We also mention some papers dealing numerically with a Hamiltonian in the planetary mechanics context (see Ollé and Pacha, 1999) and in the galactic one (see Pfenniger, 1985b; Pfenniger, 1990; Contopoulos and Barbanis, 1994; Ollé and Pfenniger, 1998).

The aim of this paper is thus to show such bifurcation and the intricate dynamics related to it, for the vertical family of periodic orbits of the triangular points of the RTBP with $\mu > \mu_R$. This will be done from the numerical point of view, without any reduction to normal form. In this sense, let us point that a rigorous identification of the character of the bifurcation (direct or inverse) forces to do a nonlinear analysis of the normal form, but, from the numerical point of view, we will show the direct character by studying the stability of the bifurcated $2D$ tori.

The contents of the paper are organized as follows. In Section 2 we introduce the vertical family of periodic orbits and discuss its linear character, showing it to be a natural candidate to have the transition stability-complex instability. Section 3 shows the typical behaviour of the bifurcation in the rational case. In Section 4 we explore the irrational collision: on the one hand, the numerical computation and evolution of the $2D$ invariant tori as well as the stable and unstable $2D$ invariant manifolds of the complex unstable periodic orbit are described. On the other hand, the consequences of the bifurcation on the dynamics close to the periodic orbits before, at and after the transition are shown. In particular a strong confinement close to the hyperbolic periodic orbits and a change of topology on the nearby $3D$ tori are also described.

2. Linear Stability of the Vertical Family of Periodic Orbits of L_4

The circular spatial restricted three-body problem (RTBP) describes the motion of a particle in a $3D$ (position) space under the gravitational attraction of two bodies (called primaries); we assume that the particle has negligible effect on the motion of the primaries, and that they describe circular orbits around their common center of mass (the origin of coordinates). It is usual to describe this problem in a rotating (synodical) system of coordinates such that, in suitable units of distance, mass and time, the primaries have masses $\mu \in (0, 1/2]$ and $1-\mu$, and are fixed at the points $(\mu - 1, 0, 0)$ and $(\mu, 0, 0)$. Denoting by (x, y, z) the position of the massless particle in the synodical system, we define the corresponding momenta as $p_x = \dot{x} - y$, $p_y = \dot{y} + x$ and $p_z = \dot{z}$. Then, the equations of motion for the particle can be written as an autonomous Hamiltonian system of three degrees of freedom, whose Hamiltonian reads (see Szebehely, 1967)

$$H(x, y, z, p_x, p_y, p_z) = \frac{1}{2}(p_x^2 + p_y^2 + p_z^2) + yp_x - xp_y - \frac{1-\mu}{r_1} - \frac{\mu}{r_2} \qquad (1)$$

r_1 and r_2 being the distances between the particle and the big and small primaries respectively, that is, $r_1^2 = (x-\mu)^2 + y^2 + z^2$ and $r_2^2 = (x-\mu+1)^2 + y^2 + z^2$.

It is well known that the RTBP has five equilibrium points: $L_{1,2,3}$, the so called Eulerian or collinear points (which lie on the x axis) and $L_{4,5}$, the Lagrangian or triangular points, each of which form an equilateral triangle with the primaries in the (x, y) plane, that is, they are located at points $L_{4,5} = (\mu - \frac{1}{2}, \pm\frac{\sqrt{3}}{2}, 0)$ (in the position space). As the motion around L_4 and L_5 is symmetric, we will concentrate on the point L_4.

The Jacobian matrix at the triangular points has the characteristic exponents

$$\lambda_1 = i, \quad \lambda_{2,3} = \sqrt{-\frac{1}{2} \pm \frac{1}{2}\sqrt{1 - 27\mu(1-\mu)}}, \tag{2}$$

and $\lambda_{j+3} = -\lambda_j$, $j = 1, 2, 3$. The pair $\pm i$ gives rise to vertical oscillations with angular frequency equal to 1; and we also recall that the characteristic exponents are purely imaginary and different for $0 < \mu < \mu_R = \frac{1}{2}(1 - \sqrt{23/27}) \approx 0.03852$ (Routh's mass parameter) and L_4 is linearly stable. For $\mu = \mu_R$ the planar frequencies collide on the imaginary axis; this produces a change in the linear stability and for $\mu_R < \mu \leqslant 1/2$, L_4 becomes complex-unstable.

On the other hand, for any value of the mass parameter $0 < \mu \leqslant 1/2$, the linear vertical oscillations associated with the pair $\pm i$ become a family of periodic orbits of the RTBP (due to Lyapunov's center Theorem, see Siegel and Moser, 1971): the so called vertical family of L_4. This family can be locally parametrized by its vertical amplitude or by the value of $\dot{z}$ when the orbit cuts the hyperplane $z = 0$ in positive sense.

For a given value of μ, we have used the arc step method (see for instance Belbruno et al., 1994; Simó, 1998; Gómez et al., 2001) for the numerical computation and continuation of the vertical family of periodic orbits. Actually, such family is regarded as a family of fixed points of a $4D$ suitable Poincaré maps defined by $P_h : \Sigma_h \to \Sigma_h$, where $\Sigma_h = \{(x, y, z, p_x, p_y, p_z) \in \mathbb{R}^6 | z = 0\} \cap \{H = h\}$ and $P_h(p) = q$, with $p, q = (x, y, p_x, p_y) \in \Sigma_h$ such that the solution of the $3D$ RTBP, starting at p, crosses the Poincaré section at the second passage. We remark that – abusing notation – we will represent points in Σ_h, for fixed h, with only four coordinates, as we have $z = 0$ and p_z is obtained from x, y, p_x, p_y.

Concerning the stability of the periodic orbits of the vertical family, we note that if $\mu \neq \mu_R$, and at least for small vertical amplitudes, the linear stability of the periodic orbits of the family is the same as L_4. In particular, for a fixed $0 < \mu < \mu_R$, the periodic orbits (for small amplitudes) of the vertical family are linearly stable, that is, for each periodic orbit, the corresponding four nontrivial – different from one – eigenvalues $(\lambda, 1/\lambda, \sigma, 1/\sigma)$ of the monodromy matrix lie on the unit circle; however, for $\mu > \mu_R$, the periodic orbits of the vertical family are (for small amplitudes) complex

unstable, that is, the four eigenvalues leave the unit circle on a complex quadruple $(\lambda, \sigma = \bar{\lambda}, 1/\lambda, 1/\bar{\lambda} = 1/\sigma)$.

Nevertheless, the linear character may change for large enough amplitudes of the orbits, and, in fact, it does. In order to determine the stability or instability of the periodic orbits of a vertical family, we have computed – for each periodic orbit – the four nontrivial eigenvalues of the monodromy matrix, or equivalently, the stability parameters α and β (see Broucke, 1969) defined by the coefficients of the characteristic polynomial $p(z)$ of the monodromy matrix:

$$p(z) = (z-1)^2(z^4 + \alpha z^3 + \beta z^2 + \alpha z + 1),$$

and they satisfy

$$\alpha = -(\lambda + 1/\lambda + \sigma + 1/\sigma), \quad \beta = 2 + (\lambda + 1/\lambda)(\sigma + 1/\sigma).$$

We plot in Figure 1 the changes on the linear character of the orbits of the vertical families for any value of $\mu \in (0, 0.5]$ and increasing values of $\dot{z}$ ($\dot{z} = 0$ corresponds to the equilibrium point L_4); see also (Jorba and Villanueva, 1998). In this Figure we remark that, for a fixed value of $\mu > \mu_R$ (and close to μ_R), the corresponding vertical family of periodic orbits has a transition from stability to complex instability (when decreasing $\dot{z}$), therefore there will be a critical (transition, resonant) orbit for which the four eigenvalues will collide in pairs on the unit circle (that is, $\lambda = 1/\bar{\lambda} = \exp(\mathrm{i}2\pi\kappa)$). We will show in the next sections that this collision gives rise to a direct Hopf-like bifurcation pattern

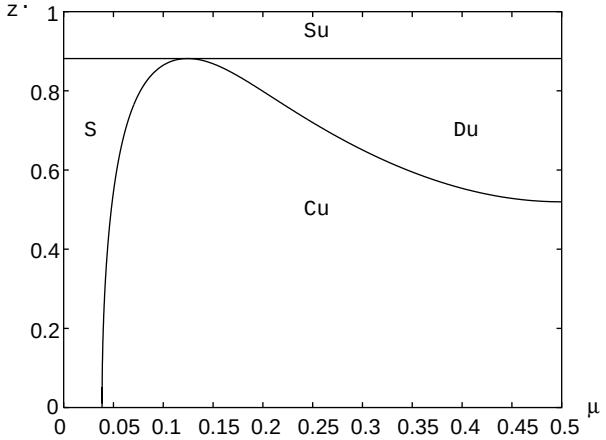

Figure 1. Change of the linear character of the orbits of the vertical family of L_4. We plot the mass parameter, μ, on the horizontal axis and the positive vertical velocity, $\dot{z}$, when $z = 0$ on the vertical one. S stands for stable (two couples of conjugate characteristic multipliers of modulus 1); Cu: complex-unstable (two conjugate eigenvalues outside the unit circle and their inverse ones); Du: double-unstable (two couples of positive eigenvalues); Su: semi-unstable (two conjugate eigenvalues of modulus 1 and a couple of positive eigenvalues).

and we will distinguish between the rational and irrational character of the collision. More precisely, we can choose suitable values of the mass parameter in order to obtain from Figure 1 critical orbits with a rational or irrational collision of multipliers. According to the value of κ, rational ($\kappa = m/n$) or irrational, then n-periodic orbits (that is, periodic orbits with a period close to n times the period of the critical orbit) or $2D$ invariant tori, respectively, may bifurcate on the unstable side (around the complex unstable periodic orbits).

3. Rational Collision

In this section we want to discuss briefly the case of rational collision and the bifurcation of n-periodic orbits linked to it (see also Pfenniger, 1985a; Bridges and Furter, 1993). In order to illustrate this phenomena, we select $\mu = 0.069608\ldots > \mu_R$ for which we have $\kappa = 1/4$ at the transition orbit, that corresponds to a rational collision.

We have computed the vertical family of L_4 for this particular value of the mass parameter. Let us denote this family by C. Figure 2 (left) shows the path of the family C on Broucke's diagram in the (α, β) plane (see also, Broucke,

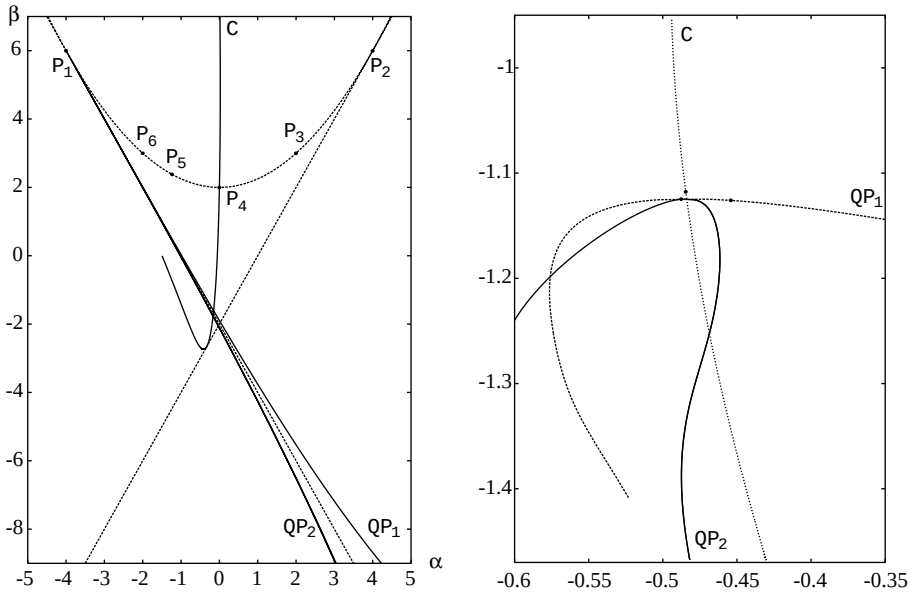

Figure 2. Left: Broucke's diagram. Stability of the vertical family C for $\mu = 0.069608\ldots$ and of the bifurcated branches QP_1, QP_2 as well. Right: Again families C, QP_1 and QP_2; on the horizontal axis we plot the value x of the initial condition (corresponding to $z = 0$ and positive $\dot{z}$); and on the vertical one the value of the energy. A member (the marked point) of each family is also chosen (see Figure 3).

1969). There the marked points $P_1, \ldots, P_6$ correspond to rational collisions $k = 1/n$ with $n = 1, \ldots, 6$ from which families of n-periodic orbits might bifurcate. In this case, the critical orbit of the family C corresponds to the point P_4. This 1/4 rational collision produces two bifurcating families of 4-periodic orbits, that we will call QP_1 and QP_2. In Figure 2 (right) we consider the (x, h) plane, being x the initial condition (corresponding to $z = 0$ and positive $\dot{z}$) and h the value of the energy; we plot the evolution of the vertical family C which starts at L_4 for $\mu = 0.069608\ldots$ and the branches QP_1 and QP_2 (which start at the critical orbit). The branch QP_1 starts with periodic orbits that are stable and then become unstable, whereas all the periodic orbits of the branch QP_2 are unstable (see also similar results for symplectic maps in Pfenniger (1985a) and Bridges and Furter, (1993). For the details concerning the computation of the bifurcating branches of periodic orbits, we refer the interested reader to Pfenniger, (1985b) and Belbruno et al., (1994), Simó (1998), Ollé and Pacha (1999). We have selected a member orbit of each family (the marked points in Figure 2 (right)) and we also plot in Figure 3 the (x, y, z) projection of each orbit. Clearly, it can be seen that the bifurcating orbits have a period close to $4T$ where T is the period of the transition orbit.

4. Irrational Collision

Let us now concentrate on the irrational collision. To illustrate the related behaviour, we take $\mu = 0.04$, and we continue numerically the vertical family starting at L_4 (and increasing values of $\dot{z}$ when $z = 0$, or equivalently increasing h). For each orbit in the family, we have computed also the

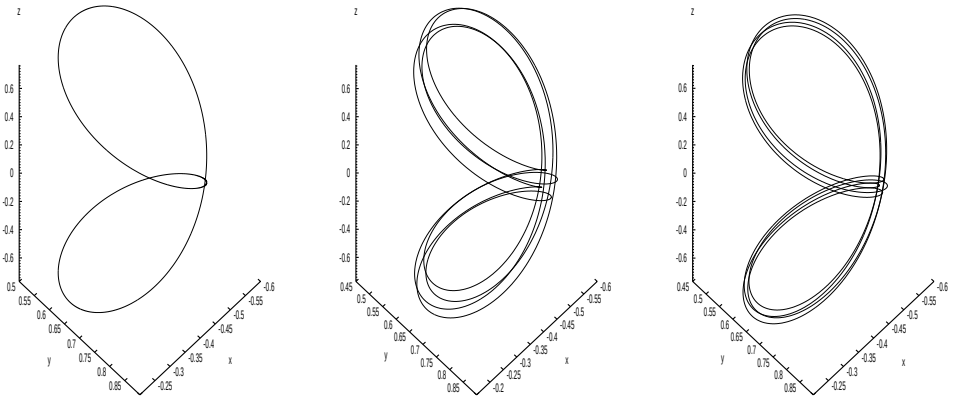

Figure 3. (x, y, z) projection of a selected orbit of each family C, QP_1 and QP_2 respectively (see Figure 2). Left: $h = -1.116234$, $T = 6.335791$; middle: $h = -1.124786$, $T = 25.337930$; right: $h = -1.1411396$, $T = 25.309643$.

associated stability parameters α, β and represented on Broucke's diagram (see Figure 4). Therein, the transition (S-CU) orbit appears, now with an irrational $\kappa = 0.291678572\ldots$ Of course, any finite decimal representation of a number is always rational. Using continuous fraction expansion we obtain that 8167/28000 is a good approximation of k which, due to the big denominator, looks quite 'irrational'. We select two orbits (one complex-unstable and one stable, marked with dots 1 and 3 in Figure 4) and we plot their (x, y, z) projection in Figure 5. We clearly see how the vertical amplitude increases as $\dot{z}$ grows.

Our aim in this section is to describe what happens around this transition. First, we summarize the results obtained: for $h > h_{\text{crit}}$, the vertical periodic orbit corresponding to this value of h is (linearly) stable, so, assuming for this orbit generic hypotheses of non resonance (involving the intrinsic frequency and the normal ones) and nondegeneracy, there are Cantorian families of $3D$ invariant tori around this orbit; there are also the two Cantorian families of elliptic $2D$ tori that are born at the periodic orbit – the so called Lyapunov families of $2D$ tori, which result from the quasiperiodic excitations of the vertical family in each of the two elliptic directions given by the normal frequencies – (see Jorba and Villanueva, 1997, 1998; Jorba and Ollé, 2004). If we restrict to $\{H = h\}$, these families of elliptic tori are both 1-dimensional. For $h = h_{\text{crit}}$, both families become one family and it detaches from the critical periodic orbit, when $h < h_{\text{crit}}$, as a single family of elliptic $2D$ invariant tori. See Figure 6. Here, we remark that when h decreases and

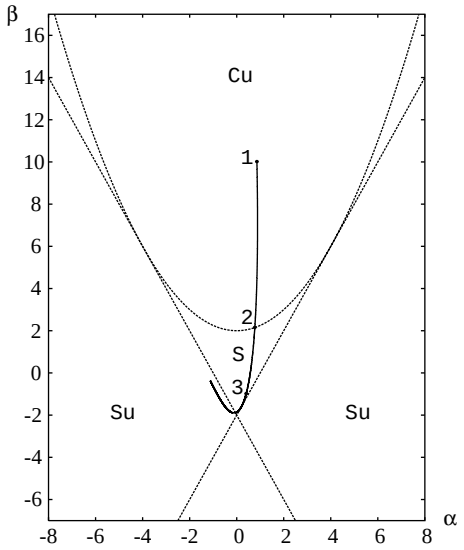

Figure 4. Broucke's diagram for the vertical family of L_4 for $\mu = 0.04$.

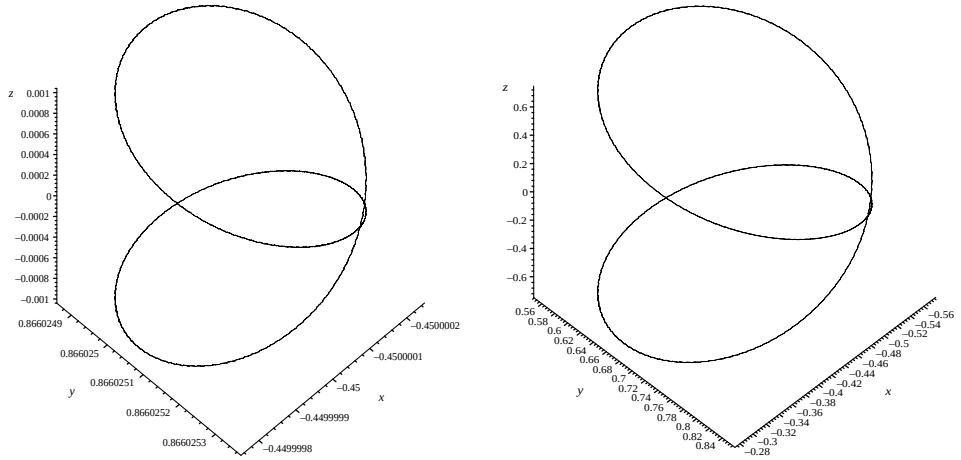

Figure 5. (x, y, z) projection of a complex unstable orbit (left) and a stable one (right) that belong to the vertical family at L_4 for $\mu = 0.04$ (see the marked points 1 and 3 on Figure 4).

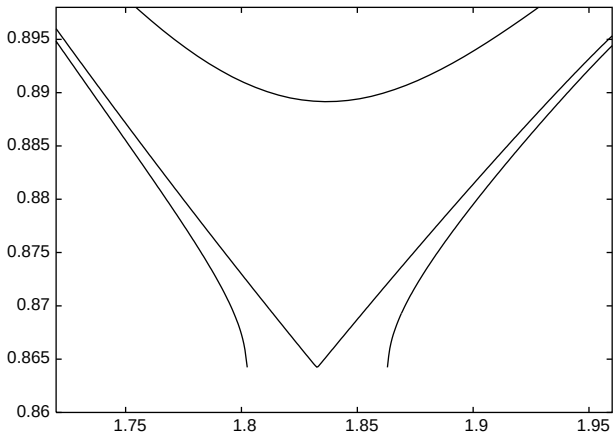

Figure 6. For $\mu = 0.04$, we plot in the $(\omega, \tilde{y})$ plane, the two Lyapunov families of invariant curves (the two lowermost – left and right – curves in the plot) for $h = -1.457018 > h_{\text{crit}}$; when h decreases up to $h = h_{\text{crit}}$, the two families meet at $(\tilde{y}_{\text{crit}}, \omega_{\text{crit}})$. We also plot the *detached* family (uppermost curve) for $h = -1.458308 < h_{\text{crit}}$. See the text for details.

crosses the critical value h_{crit}, the periodic orbit becomes hyperbolic: on the one hand, the elliptic $2D$ tori unfold on the unstable side (at a finite distance of the periodic orbit) and, on the other hand, the $3D$ unstable and stable invariant manifolds of each periodic orbit of the family become almost coincident (when h is very close to and less than h_{crit}) and as a consequence, the motion is confined for a very long time in a small neighbourhood of the unstable periodic orbit. The just described pattern of motion is known as the

direct Hamiltonian–Hopf bifurcation in dimension three (see Bridges et al., 1995; Ollé et al., 2001; Pacha 2002), and it resembles the standard (direct) Hopf bifurcation in dimension two, where an elliptic periodic orbit detaches from the equilibrium point when this equilibrium point becomes unstable.

In the following subsections we will show this behaviour in detail.

4.1. PARAMETRIZATION AND NUMERICAL COMPUTATION OF INVARIANT CURVES

First, we want to study the behaviour of $2D$ tori (in the flow context), so we will compute the corresponding invariant curves for the Poincaré map (see definitions in Section 2). We will assume, throughout the paper, that an invariant curve with frequency $\omega \notin 2\pi\mathbb{Q}$ can be parametrized by $\theta \in \mathbb{T}^1 = \mathbb{R}/2\pi\mathbb{Z} \mapsto X(\theta) \in \Sigma_h$ such that

$$P_h(X(\theta)) = X(\theta + \omega).$$

We remark that if (ω_1, ω_2) is a suitable vector of frequencies of the 2-dimensional torus, for the flow, then $\omega = 2\pi\omega_1/\omega_2$ for the map. Equivalently, let $C(\mathbb{T}^1, \mathbb{R}^4)$ denote the space of continuous functions from $\mathbb{T}^1$ to $\mathbb{R}^4$; then $X(\theta)$ is a zero of the functional $F : C(\mathbb{T}^1, \mathbb{R}^4) \to C(\mathbb{T}^1, \mathbb{R}^4)$ defined by

$$F(X)(\theta) = P_h(X(\theta)) - X(\theta + \omega).$$

The numerical method used to compute invariant curves has already been described in the flow context in Castellá and Jorba, (2000) and for mappings in Ollé (2000), Jorba (2001) and Jorba and Ollé, (2004). We just recall that if we write $X(\theta)$ as a real Fourier series,

$$X(\theta) = a_0 + \sum_{k>0} (a_k \cos(k\theta) + b_k \sin(k\theta)), \quad k \in \mathbb{N}, \quad a_k, b_k \in \mathbb{R}^4$$

then we should determine the Fourier coefficients such that they verify the equation $F(X) = 0$. Actually we compute (numerically) a truncation of this series, that is

$$X_N(\theta) = a_0 + \sum_{k=0}^{N} (a_k \cos(k\theta) + b_k \sin(k\theta)), \quad N \in \mathbb{N},$$

($N \leqslant 50$ in our computations) and we determine the $2N + 1$ unknown coefficients a_0, a_k, b_k (in $\mathbb{R}^4$) as a solution of the discretized version of the equation $F(X) = 0$ obtained when we impose that the equation $F(X_N) = 0$ is satisfied only at the mesh of $2N + 1$ points on $\mathbb{T}^1 : \theta_j = \frac{2\pi j}{2N+1}$, $0 \leqslant j \leqslant 2N$.

Let us remark finally that if $X(\theta)$ is a Fourier series corresponding to an invariant curve then, for any $\psi \in \mathbb{T}^1$, $Y(\theta) \equiv X(\theta + \psi)$ is a different Fourier series (i.e. with different Fourier coefficients) corresponding to the same invariant curve as $X(\theta)$. This introduces numerical difficulties when taking the linear system obtained and one applies the Newton method to solve the

equation $F(X_N) = 0$. In order to avoid this problem, we simply add an extra condition imposing that a component of $X(\theta)$ has a prescribed value when $\theta = 0$. This will overcome the lack of uniqueness problem.

4.2. HOPF BIFURCATION OF A FAMILY OF INVARIANT CURVES

It is well known that if the eigenvalues (also called characteristic multipliers) of the monodromy matrix associated with a periodic orbit are λ_i, for $i = 1, \ldots, 6$, with $\lambda_5 = \lambda_6 = 1$, then the eigenvalues of the differential of the Poincaré map, DP_h at a fixed point are $\gamma_i = \lambda_i, i = 1,2,3,4$. For $h > h_{\text{crit}}$, the periodic orbit of the vertical family is (linearly) stable, therefore, the eigenvalues of the matrix DP_h at the corresponding fixed point are given by $\lambda_{1,2} = \exp(\pm \mathrm{i}\omega_1)$, $\lambda_{3,4} = \exp(\pm \mathrm{i}\omega_2)$. The linear dynamics around this fixed point is given by the product of two harmonic oscillators, and it is proved that (under generic KAM conditions) each linear oscillation gives rise to a Cantorian 1-parametric family of invariant curves with a frequency that tends to $\omega_i, i = 1, 2$, when the invariant curves tend to the fixed point (see Jorba and Villanueva, 1998). We refer to these two families as Lyapunov families of invariant curves – $2D$ tori for the flow itself – (see also Jorba and Villanueva, 1998; Jorba and Ollé, 2004).

For each invariant curve computed we consider its parametrization $X(\theta)$, its frequency ω and the initial point $X(0) = (\tilde{x}, \tilde{y}, \tilde{p}_x, \tilde{p}_y)$; for all the invariant curves we fix the value of $\tilde{x}$ (as explained above) and we take $\tilde{x} = -0.462$ (close to the value $x = \mu - \frac{1}{2}$ of the point L_4). In order to represent each invariant curve, we consider two coordinates $(\omega, \tilde{y})$; therefore, a family of invariant curves may be regarded as a curve in the plane $(\omega, \tilde{y})$.

We compute several families of invariant curves to show the direct Hopf bifurcation pattern. Actually, these are Cantorian families of invariant curves, but the holes are too small to be detected with the standard double precision arithmetic of the computer; so, from the numerical point of view, we deal with these families as if they were continuous. Figure 6 shows the two Lyapunov families of invariant curves (in the plane $(\omega, \tilde{y})$) for a fixed $h = -1.457018 > h_{\text{crit}}$ (the lowermost – left and right – curves in the figure): for this value of h, the corresponding periodic orbit has $\tilde{y} = 0.86385432$ and its normal frequencies are $\omega_1 = 1.8028458$ and $\omega_2 = 1.8625327$; so, each family of invariant curves is born at the same periodic orbit (the same value of $\tilde{y}$) but with the associated $\omega_i, i = 1, 2$.

As mentioned above, when h decreases and tends to $h_{\text{crit}} = 1.45714146$, the two normal frequencies tend to collide, and at the critical orbit we have $\tilde{y} = \tilde{y}_{\text{crit}} = 0.86386304$ and $\omega = \omega_{\text{crit}} = 2\pi\kappa = 1.8326287$; therefore the two families get closer and become a single family for $h = h_{\text{crit}}$. For $h < h_{\text{crit}}$, this

family detaches from the periodic orbit in the sense that the family of invariant curves exists at a finite (and different from zero) distance from the periodic orbit which now is complex unstable. We see the evolution of this single family in Figure 6 for $h = -1.458308 < h_{\text{crit}}$; as h decreases the distance of the invariant curves to the periodic orbit increases.

We also show in Figure 7 (left) an invariant curve of the Lyapunov family near the stable vertical periodic orbit ($h = -1.457018, \omega = 1.93$) and another one of the family on the unstable region for the same value of ω and $h = -1.458308$. If we follow the flow, the corresponding $2D$ tori are plotted in Figure 7 (right).

4.3. LINEAR NORMAL BEHAVIOUR AROUND THE INVARIANT CURVES

Now we assume that $\theta \in \mathbb{T}^1 \to X(\theta) \in \Sigma_h$ is an invariant curve with frequency ω of the Poincaré map P_h. Then its linearized behaviour is described by the 4-dimensional dynamical system

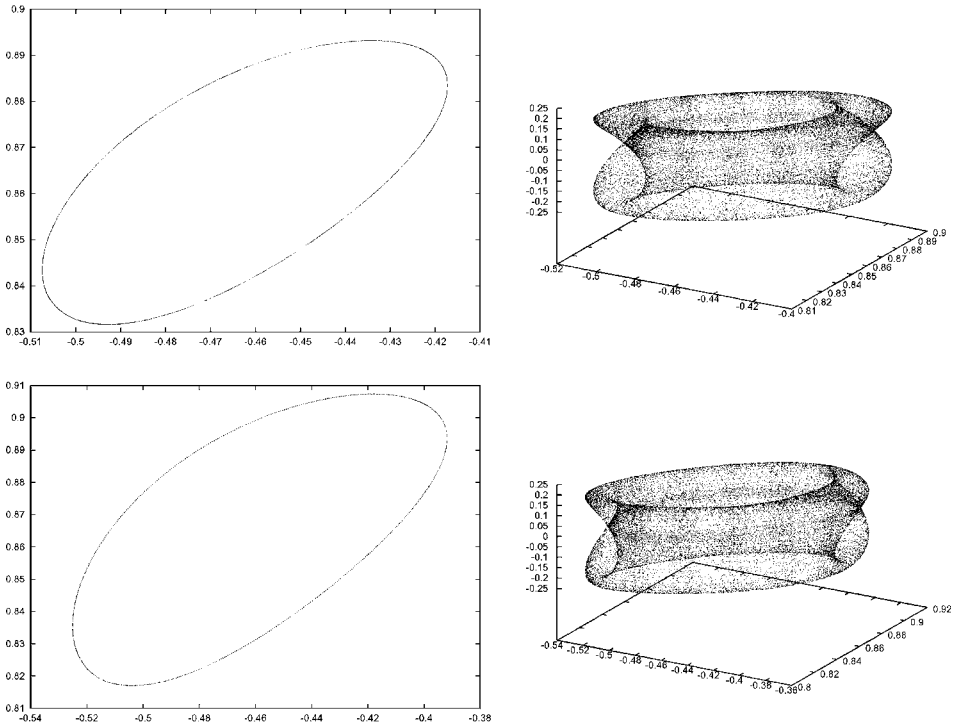

Figure 7. $\mu = 0.04$. $2D$ torus of the Lyapunov family of invariant tori on the stable region (top, with $\omega = 1.90052495$) and on the complex unstable zone (bottom, with $\omega = 1.79602495$). Left: (x, y) projection of the invariant curve in the Poincaré section $z = 0$. Right: (x, y, z) projection of the corresponding torus under the flow.

$$\left.\begin{aligned}\overline{X} &= A(\theta)X\\ \bar{\theta} &= \theta+\omega\end{aligned}\right\}, \tag{3}$$

where $A(\theta) = DP_h(X(\theta))$. This kind of system is sometimes known as linear quasi-periodic skew-product.

The system (3) is called reducible if there exists a 2π periodic (and maybe complex) change of variables $X = C(\theta)Y, \theta \in \mathbb{T}^1$, such that (3) becomes

$$\left.\begin{aligned}\overline{Y} &= BY\\ \bar{\theta} &= \theta+\omega\end{aligned}\right\}, \tag{4}$$

where the matrix $B \equiv C^{-1}(\theta+\omega)A(\theta)C(\theta)$ does not depend on θ. Of course the dynamics of (4) can be easily described by computing the eigenvalues of B. As we do not know a direct method to compute the matrix $C(\theta)$, we will consider an alternative method to compute the spectrum of B.

Let us discuss the general n-dimensional case. Given $\psi \in C(\mathbb{T}^1, \mathbb{C}^n)$, we define the linear operator L_ω by

$$(L_\omega\psi)(\theta) = A(\theta-\omega)\psi(\theta-\omega). \tag{5}$$

It turns out that the reducibility of (3) can be characterized in terms of the spectrum of L_ω. That is, we first solve numerically the generalized eigenvalue problem

$$(L_\omega\psi)(\theta) = \lambda\psi(\theta), \tag{6}$$

and afterwards we take into account the following properties (the details and proofs can be found in Jorba, (2001)):

PROPOSITION 1. *Let $\lambda \in \mathbb{C}$ be an eigenvalue of L_ω. Then, for any $k \in \mathbb{Z}$, $\lambda\exp(\mathrm{i}k\omega)$ is also an eigenvalue of L_ω.*

DEFINITION 1. Two eigenvalues λ_1 and λ_2 of L_w are said to be ω-unrelated if $\lambda_1 \neq \lambda_2\exp(\mathrm{i}k\omega)$ for all $k \in \mathbb{Z}$.

PROPOSITION 2. *Assume that there exists n ω-unrelated eigenvalues $\lambda_1 \ldots, \lambda_n$ for L_ω.* Then (3) can be reduced to (4), where $B = \mathrm{diag}(\lambda_1 \ldots, \lambda_n)$.

From these results we conclude that an alternative way to compute the eigenvalues of B is to approximate numerically the spectrum of L_ω. We have followed this approach in this paper since we know that most of the invariant curves computed are reducible, that is, the corresponding linear dynamical system (3) is reducible (see Jorba and Villanueva, 1997; Pacha, 2002).

In particular, Proposition 1 implies that the eigenvalues of the operator L_ω fill densely circles centered at the origin, and since we are in a Hamiltonian context, we remark that B is a symplectic matrix therefore its eigenvalues are

$1, 1, \lambda, 1/\lambda$. So an easy way to numerically determine the elliptic or hyperbolic character of an invariant curve is the following: we state that the invariant curve will be (linearly) stable if the eigenvalues of the operator L_ω lie on the unit circle of radius one, and unstable if the closure of the eigenvalues are three circles of radius one, $0 < c < 1$ and $1/c$.

In order to implement numerically these results, we need a procedure to approximate the solutions of the generalized eigenvalue problem (6). The computations are based on the same discretization used in Subsection 4.1 to compute invariant curves. Given a truncation value N, it is not difficult to derive the matrix (of dimension $4(2N + 1)$) which represents the truncation of L_ω. Finally, the eigenvalues and eigenvectors of this matrix are computed by a standard numerical procedure. As an example we consider an invariant curve of the family with $h = -1.457018$, and we show in Figure 8 the eigenvalues (in the complex plane) of the associated discretized operator L_ω for a truncation value $N = 8$ (Figure 8 (left)) and $N = 50$ (Figure 8 (right)). Since the eigenvalues lie on the unit circle, we conclude that this invariant curve is (linearly) stable.

It is also possible to derive heuristic estimates on the truncation error of the eigenfunctions from the decay of their Fourier coefficients and their size at the truncation point. Therefore, it is also possible to select, among the computed eigenfunctions, the most accurate ones – and, hence, the most accurate representants of the classes of ω-related eigenvalues – for the actual truncation. We refer to Jorba (2001) for a more complete description of these ideas and procedures.

This computation of the normal behaviour has been carried out for all the Lyapunov families of invariant curves obtained and they turn out to be (linearly) stable (i.e. the eigenvalues of the corresponding matrix B are $1, 1, \lambda = \exp(\mathrm{i}\delta)$ and $1/\lambda$). Therefore we conclude that the Lyapunov families of (linearly) stable

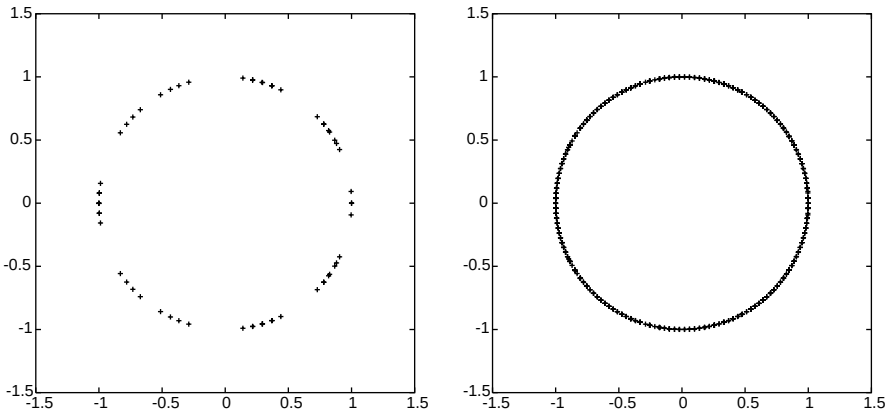

Figure 8. Eigenvalues of the discretized operator for $N = 8$ (left) and $N = 50$ (right).

invariant curves persist on the unstable side (around the complex unstable periodic orbits) and they remain (linearly) stable. That is, we conclude that the irrational collision gives rise to the direct Hopf bifurcation pattern.

4.4. DYNAMICS IN THE NEIGHBOURHOOD OF THE PERIODIC ORBITS CLOSE TO THE TRANSITION

A natural question that arises is about the consequences –concerning the dynamics– of such direct Hopf bifurcation in the neighbourhood of the family of periodic orbits close to the transition. In summary, we mention the following two features: the existence of the stable and unstable manifolds of the complex unstable periodic orbits produce a powerful confinement on the motion close to such periodic orbits. At the same time, the bifurcating elliptic $2D$ tori on the hyperbolic side give rise to secondary tori ($3D$ tori close to the periodic orbits – after the transition to complex instability) with a different topology from the $3D$ KAM tori. We describe the details below.

4.4.1. *Invariant manifolds of the complex unstable periodic orbits*

Let us show the behaviour of the invariant manifolds – which are 3-dimensional – of the complex unstable periodic orbits. In order to approximate them numerically we regard again a periodic orbit as a fixed point of the Poincaré map P_h and we compute the 2-dimensional invariant manifolds (in the map context) of this fixed point. So, let us fix the value of $H = h < h_{\text{crit}}$ and let $p = (x_0, y_0, p_{x_0}, p_{y_0}) \in \Sigma_h$ be the fixed point associated with the complex unstable periodic orbit. We compute the eigenvalues of the differential of the Poincaré map, DP_h, at the fixed point p; they are, $\lambda_{1,2} = r_{1,2}\exp(-\mathrm{i}\omega)$, with $0 < r_1 < 1, r_2 > 1$ and $\lambda_{3,4} = r_{1,2}\exp(\mathrm{i}\omega), \omega \in \mathbb{R}$. In order to approximate the unstable manifold of the fixed point p, we first select the eigenvalue λ_2 and we denote by $u + iv$ (u and v are unitary vectors in $\mathbb{R}^4$) the associated eigenvector. As it is well known, the plane generated by u and v is a linear approximation to the $2D$ real unstable manifold, therefore it is a good approximation to the manifold in a small neighbourhood of the point. As we want to see how this manifold evolves also outside this small neighbourhood, we consider the closed curve – called from now on the initial curve – on the linear approximation to the manifold given by $(x_0, y_0, p_{x_0}, p_{y_0}) + \sigma(s)$, with $\sigma(s)$ defined by

$$\sigma(s) = c\frac{\tilde{\sigma}(s)}{||\tilde{\sigma}(s)||}, \qquad \text{where} \qquad \tilde{\sigma}(s) = \cos(s)u + \sin(s)v, \quad s \in [0, 2\pi], \tag{7}$$

and c is a small quantity. In order to see how the manifold behaves, we compute the iterates – through the map P_h – of this curve (following the flow for fixed h).

We remark that the same computation can be done for the stable manifold, taking the eigenvalue λ_1, the corresponding eigenvector and following the flow through negative time; therefore using the map P_h^{-1}.

As an example, we consider the hyperbolic periodic orbit with $h = -1.4577796221 < h_{\text{crit}}$ and the initial curve (7) on the unstable manifold. We compute the iterates (by means of P_h) of this initial curve and in Figure 9 (left) we plot the kth iterate ((x, y) projection) for $k = 100$, 200 and 300. These curves (all of them belonging to the unstable manifold) show the

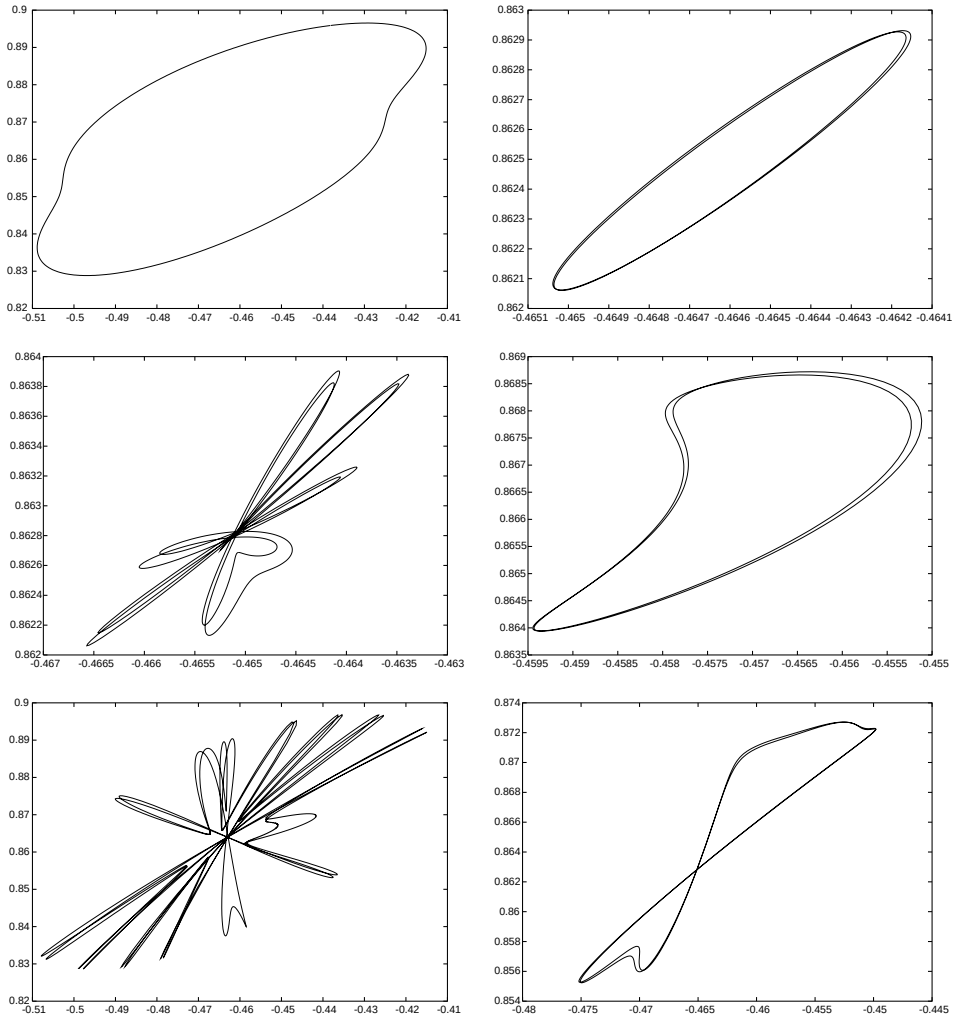

Figure 9. $\mu = 0.04$. (x, y) projection of the k-iterate, using P_h, of the initial curve (7) on the unstable (left) and stable (right) manifolds of the complex periodic orbit with $h = -1.4577796221 < h_{\text{crit}}$. Top: $k = 100$, middle: $k = 200$ and bottom: $k = 300$.

intricate to and fro behaviour of the iterates on the invariant manifolds: the iterates go far away and then back (close) to the fixed point, repeatedly, in a chaotic way. A similar computation is done for the stable manifold (see Figure 9 (right)).

Another numerical approach to show that the invariant manifolds go far away and come back is by means of slices of the manifolds: given, as above, the fixed point $p = (x_0, y_0, p_{x_0}, p_{y_0}) \in \Sigma_h$ (corresponding to the hyperbolic periodic orbit), we compute the slice of the invariant manifold defined by $x = x_0$. This slice turns out to be a curve and we plot (a piece of) it in Figure 10 for the invariant unstable manifold (left) and for the stable one (right) of the complex unstable periodic orbit used in Figure 9; apparently both slices coincide but they do not. This happens since we have only plotted the slice obtained when the unstable manifold leaves the fixed point and goes back near it for the first time. Actually, we know from the analytical results (see Pacha, 2002; Ollé et al., in press), that if we consider the truncated and integrable normal form of the Hamiltonian around the critical orbit, then the unstable and stable invariant manifolds of a complex unstable periodic orbit coincide; however, when the complete (nonintegrable) Hamiltonian is regarded (that is, the truncated normal form plus the remainder), the splitting of separatrices appears and this produces the chaotic behaviour of the iterates on the invariant manifolds observed in Figure 9.

4.4.2. *Confinement and 3D tori*

On the one hand, the almost coincidence of the manifolds somewhat trap the motion inside them giving rise to a powerful confinement in the sense that a point close to the unstable (or stable) manifold may follow the shape of the manifolds and remain confined near them for a long time (many iterates in the map context).

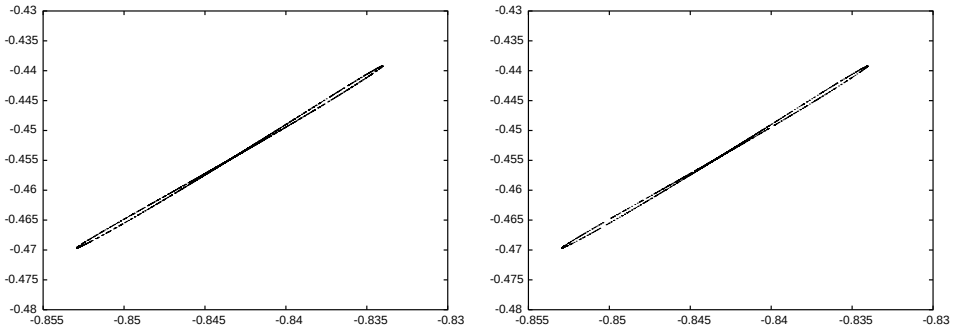

Figure 10. $\mu = 0.04$. (p_x, p_y) projection of the slice $x = x_0$ (see the text) of the invariant unstable (left) and stable (right) manifolds of the complex unstable periodic orbit of Figure 9.

In order to show this behaviour, we consider the evolution of a $2D$ KAM torus in Σ_h ($3D$ torus in the flow context) before, at and after the transition. For $h = -1.44908826 > h_{\text{crit}}$, the fixed point (periodic orbit for flows) is stable so there are plenty of $2D$ KAM tori; we plot in Figure 11 (top left) the 5000 iterates – through P_h – of an initial condition of a $2D$ torus near the stable fixed point. In Figure 11 (top right), we do the same computation for $h = h_{\text{crit}} = -1.45714146$; we remark now the bigger size in the plot window since for $h < h_{\text{crit}}$ the fixed point becomes complex unstable and its invariant manifolds play a key role. For $h = -1.45777962 < h_{\text{crit}}$, we consider the corresponding hyperbolic fixed point $p = (x_0, y_0, p_{x_0}, p_{y_0})$ and we take initial conditions $\bar{p} = (x_0 + \epsilon, y_0 + \epsilon, p_{x_0} + \epsilon, p_{y_0} + \epsilon)$ (for $\epsilon > 0$ small) close to it. We plot the 20,000 iterates (using P_h) in Figure 11 (bottom left with $\epsilon = 10^{-6}$, and bottom right with $\epsilon = 10^{-4}$). We remark again the even bigger size of both plots window since there do exist invariant manifolds in this case; we observe in Figure 11 (bottom left) how the iterates follow the invariant manifolds shape and describe a chaotic orbit; actually the same picture is obtained if we plot the iterates of a point in the unstable manifold. On the

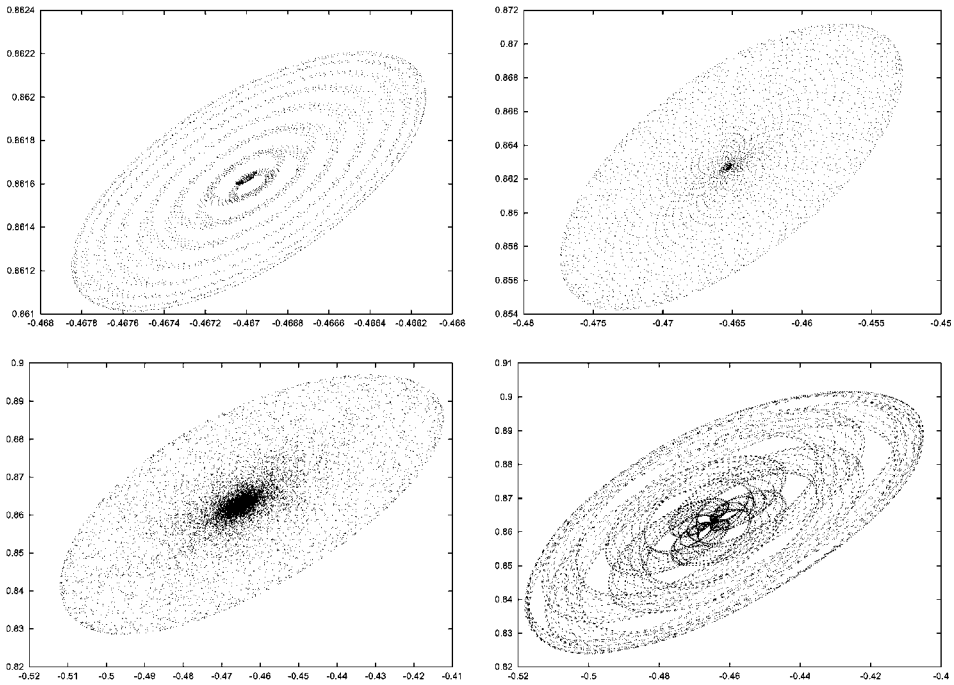

Figure 11. 5000 iterates ((x, y)-projection) of initial conditions on a $2D$ torus close to a stable (top left) and critical (top right) fixed point. 20,000 iterates of the initial condition $\bar{p}$ (see the text) close to a complex unstable periodic orbit; $\epsilon = 10^{-6}$ (bottom left) and $\epsilon = 10^{-4}$ (bottom right). We remark the different size for the frame in each case.

other hand, for a bigger value of $\epsilon = 10^{-4}$, the iterates in Figure 11 (bottom right) seem to remain in a $2D$ torus (either one $2D$ KAM torus that survives the bifurcation or a secondary $2D$ torus which is born from the existence of the stable bifurcating invariant curves); in any case, however, the k-iterates are confined for a large value of k.

We remark finally that, if the iterates are on a $2D$ torus, they would be confined forever; but also Arnol'd diffusion (see Arnol'd, 1964) may appear since the system is non integrable. However, due to the strong confinement of the trajectories we can expect long time (maybe not for exponential times as we are close to a resonant orbit) effective stability estimates (Nekhoroshev's estimates). In this context, we mention reference Ollé and Pfenniger (2000) where some numerical Nekhoroshev's type estimates of diffusion have been carried out for a particular $4D$ symplectic mapping undergoing a transition from stability to complex instability.

On the other hand, we also remark that the effect of the bifurcation is local in the following sense: concerning the $3D$ KAM tori (in the flow context) existing around a stable periodic orbit (before the transition), two different behaviours have been shown in Figure 11: those tori close enough to the periodic orbit are sensitive to the bifurcation and they change the topology after the transition, since the $2D$ bifurcating stable tori (after the transition) give rise to the secondary $3D$ tori which have nothing to do with the KAM tori before the transition. Nevertheless, the $3D$ KAM tori far enough from the periodic orbit remain just after the transition as they are; however, as soon as the energy decreases, the invariant manifolds also increase and may reach the further $3D$ tori anyway.

Acknowledgements

This work has been partially supported by the Catalan CIRIT Grant 2001SGR-70 and the Spanish MCyT/FEDER Grant BFM2003-07521-C02-01.

References

Arnol'd, V. I.: 1964, 'Diffussion of dynamical systems with several degrees of freedom', *Sov. Math. Dokl.* **5(3)**, 581–585.

Belbruno, E., Llibre, J. and Ollé, M.: 1994, 'On the families of periodic orbits which bifurcate from Sitnikov motions', *Cel. Mech. Dynam. Astron.* **60**, 99–129.

Bridges, T. J., Cushman, R. H. and Mackay, R. S.: 1995, 'Dynamics near an irrational collision of eigenvalues for symplectic mappings', *Fields. Inst. Commun.* **4**, 61–79.

Bridges, T. J. and Furter, J. E.: 1993, 'Singularity theory and equivariant symplectic maps', *Lecture Notes in Mathematics*, Vol. 1558, Springer-Verlag.

Broucke, R.: 1969, 'Stability of periodic orbits in the elliptic restricted three-body problem', *AIAA* J. **7**, 1003–1009.

Castellà, E. and Jorba, A.: 2000, 'On the vertical families of two-dimensional tori near the triangular points of the bicircular problem', *Cel. Mech. Dynam. Astron.* **76**, 35–54.

Contopoulos, G. and Barbanis, B.: 1994, 'Periodic orbits and their bifurcations in a $3D$-system', *Cel. Mech. Dynam. Astron.* **59**, 279–300.

Gómez, G., Llibre, J., Martínez, R. and Simó, C.: 2001, '*Dynamics and Mission Design Near Libration Points*', World Scientific Monograph Series in Mathematics, Vol. 2.

Heggie, D. G.: 1985, 'Bifurcation at complex instability', *Cel. Mech.* **35**, 357–382.

Jorba, A.: 2000, 'A numerical study on the existence of stable motions near the triangular points of the real Earth-Moon system', *Astron. Astrophys.* **364**, 327–338.

Jorba, A.: 2001, 'Numerical computation of the normal behaviour of invariant curves of n-dimensional maps', *Nonlinearity* **14**, 943–976.

Jorba, A. and Ollé, M.: 2004, 'Invariant curves near Hamiltonian-Hopf bifurcations of $4D$ symplectic maps', *Nonlinearity* **17**, 691–710.

Jorba, A. and Villanueva, J.: 1998, 'Numerical computation of normal forms around some periodic orbits of the RTBP', *Physica D* **114**, 197–229.

Jorba, A. and Villanueva, J.: 1997, 'On the normal behaviour of partially elliptic lower dimensional tori of Hamiltonian systems', *Nonlinearity* **10**, 783–822.

Ollé, M.: 2000, 'Numerical exploration of bifurcation phenomena associated with complex instability'. In: *Numerical Methods for Bifurcation Problems and Large-Scale Dynamical Systems*, *IMA vol. in Maths and its Applications*, *Springer Verlag*, pp. 319–326.

Ollé, M. and Pacha. J. R.: 1999, 'The 3D elliptic RTBP: periodic orbits which bifurcate from limiting restricted problems', Complex instability, *Astron. Astrophys.* **351**, 1149–1164.

Ollé, M., Pacha, J.R. and Villanueva, J.: in press, Dynamics and bifurcation near the transition from stability to complex instability. In: *Proceedings of the IV International Symposium HAMSYS-2001*. Guanajuato (México), March 19–24, 2001.

Ollé, M., Pacha, J. R. and Villanueva, J.: 2003, '*Dynamics close to a non semi-simple* 1: -1 resonant periodic orbit, preprint 2003, web site page http://www-mal.upc.es/recerca/2003.html.

Ollé, M. and Pfenniger, D.: 2000, 'Bifurcation at complex instability, In: C. Simó (ed.), *Hamiltonian systems with three or more degrees of freedom*, NATO Adv. Sci. Inst. Ser. C Math. Phys. Sci., Vol. 53, Kluwer Acad. Publ. Dordrecht, Holland, pp. 518–522.

Ollé, M. and Pfenniger, D.: 1998, 'Vertical orbital structure and the Lagrangian points in barred galaxies', *Astron. Astrophys.* **334**, 829–839.

Pacha, J. R.: 2002, *On the quasi-periodic Hamiltonian Andronov-Hopf bifurcation*, PhD thesis, UPC, Barcelona, web page site http://tdx.cesca.es.

Pfenniger, D.: 1985, 'Numerical study of complex instability'. I Mappings, *Astron. Astrophys.* **150**, 97–111.

Pfenniger, D.: 1985, 'Numerical study of complex instability'. II Barred galaxy bulges, *Astron. Astrophys.* **150**, 112–128.

Pfenniger, D.: 1990, 'Stability of the Lagrangian points in stellar bars', *Astron. Astrophys.* **230**, 55–66.

Siegel, C. and Moser, J.: 1971, *Lectures on Celestial Mechanics*, Springer-Verlag, New York.

Simó, C.: 1998, Effective computations in Celestial Mechanics and Astrodynamics, In: V.V. Rumyantsev and A.V. Karapetyan (eds), *Modern Methods of Analytical Mechanics and Their Applications*, Vol. 37 of CISM Courses and Lectures, Springer-Verlag.

Szebehely, V.: 1967, *Theory of orbits*, Academic Press, New York.
Zagouras, C. G.: 1985, 'Three-dimensional periodic orbits about the triangular equilibrium points of the restricted problem of three bodies', *Cel. Mech.* **37**, 27–46.